RSC Advances

PAPER

View Article Online
View Journal | View Issue

Cite this: *RSC Adv.*, 2018, **8**, 17321

A weaker donor shows higher oxidation state upon aggregation†

Longfei Ma, Haili Peng, Xiaofeng Lu, Lei Liu and Xiangfeng Shao *

Received 6th April 2018
Accepted 4th May 2018

DOI: 10.1039/c8ra02956c

rsc.li/rsc-advances

The charge-transfer between TTFs and I_2 shows that the stronger donor **TTF1** is in a cation radical state and the weaker donor **TTF2** is neutral in solution, whereas **TTF1** exists as a cation radical and **TTF2** is dicationic in complexes. The dicationic and neutral states of **TTF2** are reversible upon aggregation and solvation.

Charge-transfer (CT) between an electron donor and acceptor plays the pivotal role in supramolecular assembly and creation of conducting materials. There remains a challenge in CT, that is, whether a weaker donor could show a positively charged state higher than a stronger donor through the CT with the same acceptor.

Iodine (I_2) can serve as an acceptor to prepare CT complexes. The CT complex perylene–iodine is one of the earliest organic conductors.[1] Upon gaining one electron from a donor molecule, iodine would form polyiodides,[2] which show diverse structures and have received growing interest in supramolecular architectures and materials science.[3,4] Tetrathiafulvalene (TTF) is an electron donor with three reversible states, $(TTF)^0$, $(TTF)^{+\bullet}$, and $(TTF)^{2+}$.[5] TTF derivatives (TTFs) have been widely employed as building blocks for functional materials.[6] The CT complexes of I_2 and TTFs can be prepared by mixing these two species.[7] Because I_2 is not a strong acceptor, TTFs are mainly in the cation radical or partially charged state in CT complexes.[8] Ar-S-TTFs are derived from TTF by decorating four arylthio groups onto the peripheral positions (Scheme 1). Ar-S-TTFs can adjust their geometry and electronic state to adapt to a guest molecule,[9] and they form CT complexes with various acceptors such as fullerene,[10] heteropoly acid,[11] and $CuBr_2$.[12]

The structures of polyiodides depend on the nature of the counter cations,[3b] and Ar-S-TTFs can modulate the geometry and electronic state according to the guest. Therefore, the CT complex containing these two flexible components seems promising. Being continuous study on Ar-S-TTFs, herein we report the CT between Ar-S-TTFs (**TTF1** and **TTF2**) and I_2. It is found that a weaker donor **TTF2** carries the positive charge higher than a stronger donor **TTF1** in their CT complexes with I_2. Meanwhile, the iodine atoms form polyiodides with different structures in CT complexes, *i.e.*, the infinite covalent chain of $[(I_n)^-]_\infty$ in **TTF2** complex and 2-D network comprised of $(I_3)^-$ and I_2 in **TTF1** complex.

Electrochemical analysis shows that both **TTF1** and **TTF2** have two reversible redox potentials. The first redox potential ($E_{1/2}{}^1$) of **TTF2** (0.66 V *vs.* SCE in CH_2Cl_2) is higher than that of **TTF1** (0.58 V), and the second redox potentials ($E_{1/2}{}^2$) show similar tendency (Scheme 1). Therefore, as donor molecule, **TTF2** is weaker than **TTF1**. Both donors display weak absorption band at 400–500 nm due to the intramolecular CT transition,[9] whereas the cation radicals of them show broad absorption at 650–1100 nm.[11] For example, electrochemical oxidation of **TTF1** under constant potential of 0.75 V results in an absorption band in this region as proved by the spectroelectrochemical study (Fig. 1a).

By mixing **TTF1** and I_2 in CH_2Cl_2, an absorption band appears at 650–1100 nm (Fig. 1b), which is identical to that observed in the spectroelectrochemistry. The mixture of **TTF1** and I_2 in CH_2Cl_2 shows ESR signal with $g = 2.006$ (Fig. 1c). Therefore, the CT occurs between **TTF1** and I_2 in CH_2Cl_2 solution, and **TTF1** is at the cation radical state. While CT occurs between **TTF1** and I_2 in CH_2Cl_2, the thin layer chromatography reveals that the neutral **TTF1** remains in solution even though excess I_2 is added (>3 equiv.); this means I_2 cannot completely

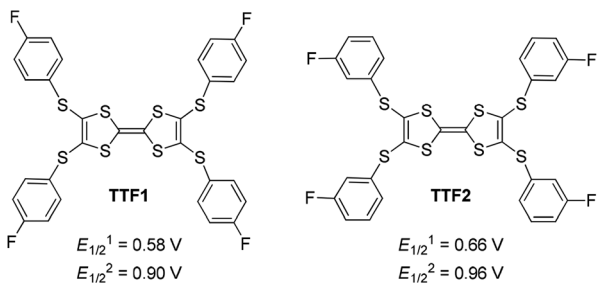

Scheme 1 Chemical structures of the Ar-S-TTFs reported herein, along with their first ($E_{1/2}{}^1$) and second ($E_{1/2}{}^2$) redox potentials in CH_2Cl_2 recorded *versus* SCE.

State Key Laboratory of Applied Organic Chemistry, Lanzhou University, Tianshui Southern Road 222, Lanzhou, Gansu Province, P. R. China. E-mail: shaoxf@lzu.edu.cn; Fax: +86 0931 8915557; Tel: +86 0931 8912500

† Electronic supplementary information (ESI) available: CCDC 1818732 and 1818736 respectively for (**TTF1**)·(I_3)·(I_2) and (**TTF2**)·(I_5)·(I_2) contain the crystallographic data. The selected crystallographic data are supplied in Table S1 in ESI. For ESI and crystallographic data in CIF or other electronic format see DOI: 10.1039/c8ra02956c

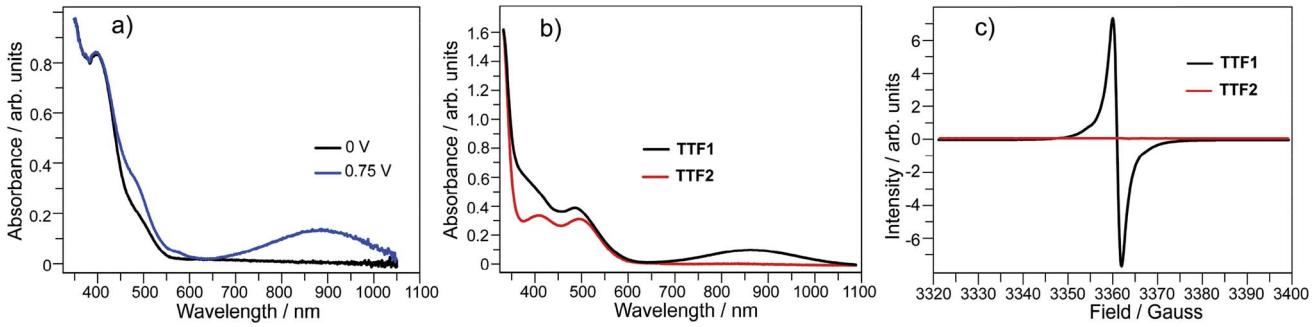

Fig. 1 (a) Spectroelectrochemistry of **TTF1** in CH_2Cl_2 ($c = 5 \times 10^{-4}$ mol L^{-1}); (b) UV-Vis absorption spectra and (c) ESR spectra of **TTF1** and **TTF2** upon adding 3 equivalents of I_2 in CH_2Cl_2 ($c = 1 \times 10^{-5}$ mol L^{-1}).

transform **TTF1** into cation radical. On the other hand, there is no CT between **TTF2** and I_2 in CH_2Cl_2 solution, because the absorbance of $(\mathbf{TTF2})^{+\bullet}$ is not observed (Fig. 1b) and the mixture of **TTF2** and I_2 is ESR inactive (Fig. 1c).

Although **TTF1** and **TTF2** exhibit the different behaviors upon mixing with I_2 in CH_2Cl_2, they both afford CT complexes with I_2. The CT complexes are obtained as black block-like single crystals by evaporating the CH_2Cl_2/*n*-hexane (v/v, 1 : 1) solution of mixture of **TTF1** (or **TTF2**) and I_2 at room temperature. The compositions of complexes are determined on the basis of single crystal structure analyses to be $(\mathbf{TTF1})\cdot(I_3)\cdot(I_2)$ and $(\mathbf{TTF2})\cdot(I_5)\cdot(I_2)$.

$(\mathbf{TTF1})\cdot(I_3)\cdot(I_2)$ crystallizes in the $P\bar{1}$ space group. There are one **TTF1** molecule and three pairs of iodine atoms (I1–I2, I3–I4, and I5–I6) in the asymmetric unit. The I3 and I5 locate on the inversion centres. The bond length of central C=C (bond *a* in Scheme 2) on TTF moiety can be used to estimate the charge on TTFs,[7] *i.e.*, 1.34 Å, 1.39 Å, and 1.45 Å respectively for $(TTF)^0$, $(TTF)^{+\bullet}$, and $(TTF)^{2+}$. Referring Fig. 2a, the central C=C bond length in **TTF1** is 1.39 Å, same to that in $(TTF)^{+\bullet}$.[7] The site charge (ρ) on TTF moiety also can be estimated *via* an empirical formula $\rho = 6.347 - 7.436\delta$,[13] where $\delta = (b + c) - (a + d)$, and *a*, *b*, *c*, and *d* are bond lengths (Scheme 2). The calculated δ-value of **TTF1** is 0.721 Å, which gives the site charge on **TTF1** to be +1. The iodine atoms (I1–I6) form three tightly connected units, [I1–I2], [I4–I3–I4], and [I6–I5–I6] (Fig. 2c). The I1–I2 bond length (2.74 Å) is identical to that of neutral I_2 (2.74 Å), and the I–I bond lengths (2.91–2.93 Å) in both [I4–I3–I4] and [I6–I5–I6] are very close to that of triiodide (2.90 Å).[14] Therefore, the [I4–I3–I4] and [I6–I5–I6] units are intrinsic $(I_3)^-$. These results indicate that **TTF1** is at cation radical state in complex, which is reasonable according to the formation of $(\mathbf{TTF1})^{+\bullet}$ in solution by mixing **TTF1** and I_2.

The **TTF1** molecules are dimerized in complex (Fig. 2b). Within a dimer, there are S···S contacts (3.45–3.53 Å) between TTF cores, and C···S contacts (3.42–3.46 Å) between the peripheral sulfur atoms and the phenyls. Meanwhile, the $(I_3)^-$ anions and neutral I_2 together form the two-dimensional (2-D) sheet *via* multiple I···I contacts (3.32–3.96 Å). The 2-D sheet is not flat but shows a zig–zag shape along the *b*-axis direction (Fig. 2d). The dimers of **TTF1** are sandwiched by the neighbouring 2-D anion sheets. There are I···S contacts (3.69–3.78 Å) between the anion sheets and **TTF1** dimers. This type of 2-D polyiodide framework is rare in the CT complexes of TTFs and I_2.[15]

$(\mathbf{TTF2})\cdot(I_5)\cdot(I_2)$ crystallizes in the *C*2/*c* space group. The asymmetric unit contains half of **TTF2**, three tightly connected iodine atoms (I1, I2, I3) with I3 on the 2-fold screw axis, and one isolated iodine atom (I4) at the general position. Referring Fig. 3a, the central C=C bond length (1.45 Å) on TTF moiety is close to that observed in the dicationic salts of Ar-S-TTFs (1.42 Å).[12] The calculated δ value of **TTF2** is 0.573 Å, giving the site charge on **TTF2** to be +2. These results firmly prove that **TTF2** is dicationic in complex, against the neutral state of **TTF2** by mixing it with I_2 in CH_2Cl_2. As shown in Fig. 3b, the I4–I4 bond length (2.79 Å) is close to that of I_2 (2.73 Å), thus the $(I4)_2$ is a neutral I_2. The I1, I2, and I3 atoms form an infinite chain with a periodicity of –[I1–I2–I3–I2–I1]–. Regarding the charge on **TTF2**, a periodic unit [I1–I2–I3–I2–I1] has a charge of −2. The interatomic distances in [I1–I2–I3–I2–I1] unit vary from 3.04 Å to 3.19 Å, almost identical to those in the infinite polymeric $[(I_n)^-]_\infty$ (3.02–3.20 Å).[3a] Therefore, the present polyiodide chain also would be a $[(I_n)^-]_\infty$ polymer, and all the iodine atoms in $[(I_n)^-]_\infty$ are partially charged.[3a] The $[(I_n)^-]_\infty$ chains are connected by $(I4)_2$ through the I···I contacts (3.42 Å) to form a ladder-like structure. The TTF cores and peripheral aryls on **TTF2** molecules together form a channel along the longitudinal axis of **TTF2** (Fig. 3c), and the channel grows through the C···S contacts (3.34–3.48 Å) between the peripheral sulfur atoms and the phenyls. The $[(I_n)^-]_\infty$ chains penetrate into the channel. It is worth noting that $[(I_n)^-]_\infty$ chain has not been observed in the complexes comprised of TTFs and polyiodide.

The charged states of **TTF1**/**TTF2** in CT complexes are further proved by the spectroscopic studies. $(\mathbf{TTF1})\cdot(I_3)\cdot(I_2)$ shows a ESR signal with $g = 2.009$ and $(\mathbf{TTF2})\cdot(I_5)\cdot(I_2)$ is ESR inactive (Fig. 4a). This is consistent with crystallographic study, *i.e.*, **TTF1** and **TTF2** are respectively at cation radical and dicationic states. The UV-Vis absorption spectra of both complexes in solid state are distinct from those of neutral **TTF1** and **TTF2** (Fig. 4b). $(\mathbf{TTF1})\cdot(I_3)\cdot(I_2)$ shows two absorption bands at the low energy

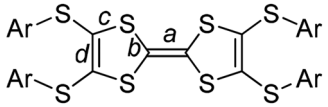

Scheme 2 The bonds (*a*–*d*) on Ar-S-TTFs for the estimation of charge ρ.

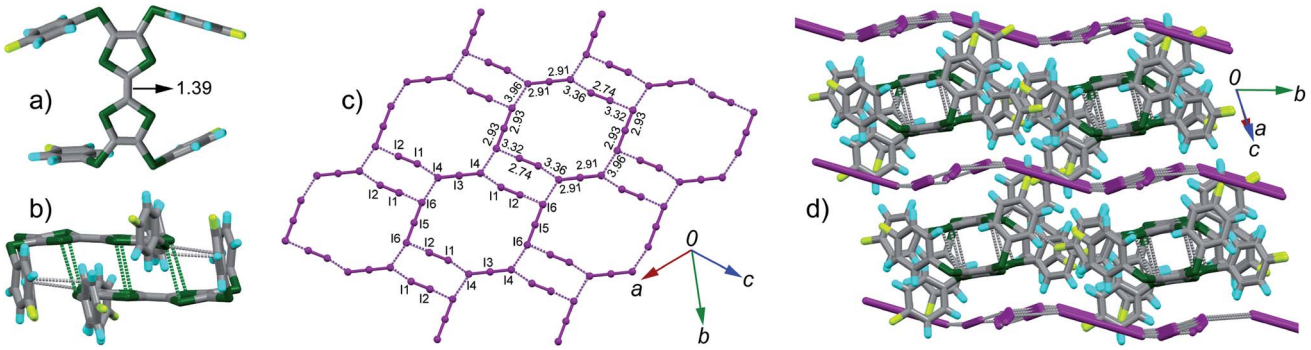

Fig. 2 Crystal structure of complex (**TTF1**)·(I_3)·(I_2): (a) top view of molecule **TTF1** with the central C=C bond length shown in unit of Å; (b) **TTF1** dimer with atomic short contacts shown in dashed lines (green for S···S and grey for C···S); (c) anion sheets composed of $(I_3)^-$ and I_2 with the I–I bond length and I···I contacts (purple dashed lines) shown; (d) packing structure viewed along the longitudinal axis of **TTF1** dimer with the I···I contacts shown in grey dashed lines.

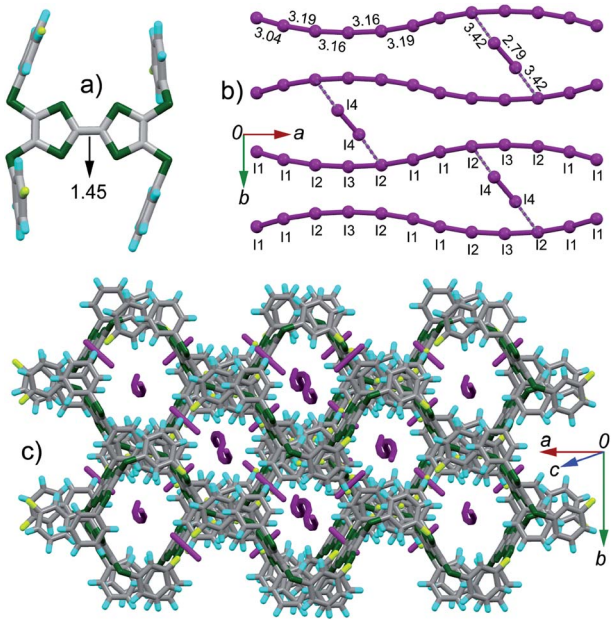

Fig. 3 Crystal structures of complex (**TTF2**)·(I_5)·(I_2): (a) top view of molecule **TTF2** with the central C=C bond length shown in unit of Å; (b) the $(I_3)^-$ anion chain with the I–I bond lengths and I···I contacts (purple dashed lines) shown; (c) packing structure projected along the longitudinal axis of the TTF moiety.

region. The band at 800–950 nm that belonging to absorbance of $(\mathbf{TTF1})^{+\bullet}$. The band at 950–1400 nm ascribable to intermolecular CT transition between the **TTF1** cation radicals in a dimer, *i.e.*, $(\mathbf{TTF1})^{+\bullet} + (\mathbf{TTF1})^{+\bullet} \rightarrow (\mathbf{TTF1})^{2+} + (\mathbf{TTF1})^{0}$.[8a] The (**TTF2**)·$(I_5)$·$(I_2)$ displays very broad absorption at 500–1400 nm, which is distinct from (**TTF1**)·(I_3)·(I_2).

As aforementioned, **TTF2** is neutral upon mixing with I_2 in CH_2Cl_2, whereas it is dicationic in (**TTF2**)·(I_5)·(I_2). Moreover, **TTF2** is a donor weaker than **TTF1**, but it shows higher oxidation state in complex. This is against to the criteria for CT between TTF and acceptor, say, the charge on TTF in CT complex depends on the oxidation potential (E_D^{ox}) of TTF and the reduction potential (E_A^{red}) of acceptor.[16] The TTF would be neutral, cation radical, and partially charged under the condition of $E_D^{ox} - E_A^{red} > 0.34$ V, $E_D^{ox} - E_A^{red} < -0.02$ V, and -0.02 V $< E_D^{ox} - E_A^{red} < 0.34$ V, respectively. In the present case, the E_A^{red} of **TTF2** is 0.69 V and the E_A^{red} of I_2 is 0.53 V (Fig. S4 in ESI†). Therefore, **TTF2** would be partially charged in CT complex. One may concern that the increment of charge transfer degree between I_2 and **TTF2** in (**TTF2**)·(I_5)·(I_2) would be attributed to the aggregation of donor and acceptor.

In this regard, the absorption spectra of complexes are studied by dissolving them in CH_2Cl_2. (**TTF1**)·(I_3)·(I_2) shows characteristic absorbance of $(\mathbf{TTF1})^{+\bullet}$ in CH_2Cl_2 (Fig. 4c), therefore the charged state of **TTF1** remain the same in solution and CT complex. On the other hand, the charge on **TTF2** is distinctly variated by dissolving (**TTF2**)·(I_5)·(I_2) in CH_2Cl_2. The **TTF2** is

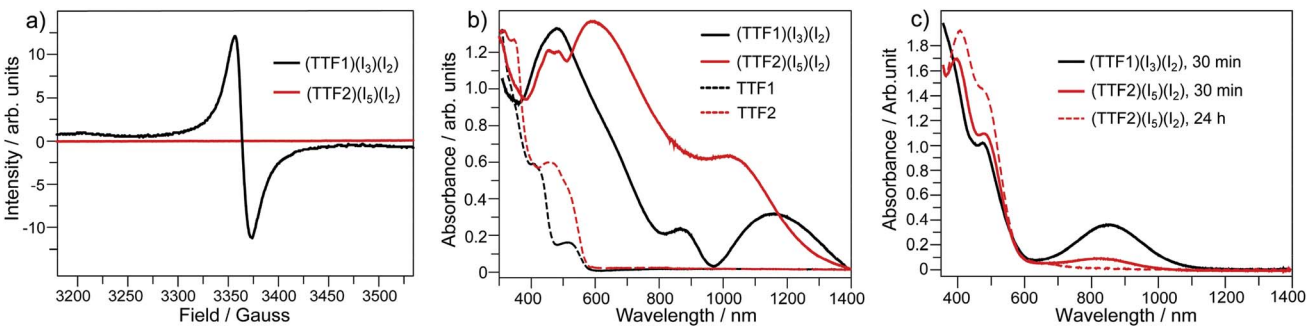

Fig. 4 (a) ESR spectra for the crystalline complexes of (**TTF1**)·(I_3)·(I_2) and (**TTF2**)·(I_5)·(I_2); UV-Vis absorption spectra of (**TTF1**)·(I_3)·(I_2) and (**TTF2**)·(I_5)·(I_2) in the (b) solid state, and (c) CH_2Cl_2 solution ($c = 10^{-5}$ mol L^{-1}) after standing under inert atmosphere for 30 min and/or 24 h.

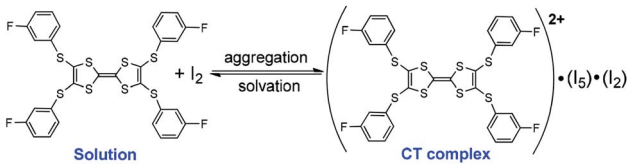

Scheme 3 Reversible process upon aggregation and solvation of (TTF2)·(I_5)·(I_2)

reduced from $(\mathbf{TTF2})^{2+}$ to $(\mathbf{TTF2})^{+\bullet}$ in 30 min as proved by an absorption band at 700–1050 nm. And, the $(\mathbf{TTF2})^{+\bullet}$ disappears to give neutral **TTF2** when the solution is kept for 24 h under inert atmosphere. This means that the retro CT occurs from $[(I_n)^-]_\infty$ to $(\mathbf{TTF2})^{2+}$ upon dissociation of $(\mathbf{TTF2})\cdot(I_5)\cdot(I_2)$, and both anionic and cationic components return to the neutral state. Moreover, the absorbance of $(\mathbf{TTF2})\cdot(I_5)\cdot(I_2)$ can be restored by evaporating the solution to gain solid complex. This process, exchanging the dicationic and neutral states of **TTF2**, is thus reversible upon aggregation and solvation of complex as shown in Scheme 3. These results prove that the dicationic state of **TTF2** in CT complex comes from the aggregation of donor and acceptor.

In summary, the CT between **TTF1**/**TTF2** and I_2 is studied in both solution and solid state. The stronger donor **TTF1** turns into cation radical and the weaker donor **TTF2** remains neutral upon mixing with I_2 in solution. On the other hand, **TTF2** shows an oxidation state (dicationic) higher than that of **TTF1** (cation radical) in their CT complexes, which is unusual for CT between TTFs and acceptors. The high oxidation state of **TTF2** in complex is due to the aggregation of donor and acceptor. The dicationic and neutral states of **TTF2** are reversible upon aggregation and solvation of CT complex. Moreover, the structures of polyiodides in CT complexes can be finely tuned by varying the aryls on Ar-S-TTFs, to give infinite $[(I_n)^-]_\infty$ and 2-D network comprised of $(I_3)^-$ and I_2. Along with previous report, this work further indicates that Ar-S-TTFs show unique feature, *i.e.*, self-modulation of electronic states and molecular geometries according to guest molecules.

Conflicts of interest

There are no conflicts to declare.

Acknowledgements

The authors acknowledge the financial support from the National Natural Science Foundation of China (21522203, 21372111).

Notes and references

1 J. Kommandeur and F. R. Hall, *J. Chem. Phys.*, 1961, **34**, 1649.
2 (*a*) P. H. Svensson and L. Kloo, *Chem. Rev.*, 2003, **103**, 1649; (*b*) A. J. Blake, W.-S. Li, V. Lippolis, M. Schröder, F. A. Devillanova, R. O. Gould, S. Parson and C. Radek, *Chem. Soc. Rev.*, 1998, **27**, 195.
3 (*a*) F. C. Küpper, M. C. Feiters, B. Olofsson, T. Kaiho, S. Yanagida, M. B. Zimmermann, L. J. Carpenter, G. W. Luther III, Z. Lu, M. Jonsson and L. Kloo, *Angew. Chem., Int. Ed.*, 2011, **50**, 11598; (*b*) Z. Yin, Q.-X. Wang and M.-H. Zeng, *J. Am. Chem. Soc.*, 2012, **134**, 4857; (*c*) J. Lin, J. Marti-Rujas, P. Metrangolo, T. Pilati, S. Radice, G. Resnati and G. Terraneo, *Cryst. Growth Des.*, 2012, **12**, 5757.
4 (*a*) S. Madhu, H. A. Evans, V. V. T. Doan-Nguyen, J. G. Labram, G. Wu, M. L. Chabinyc, R. Seshadri and F. Wudl, *Angew. Chem., Int. Ed.*, 2016, **55**, 8032; (*b*) A. Peuronen, H. Rinta and M. Lahtinen, *CrystEngComm*, 2015, **17**, 1736.
5 *TTF Chemistry: Fundamentals and Applications of Tetrahiafulvalenes*, ed. J. Yamada and T. Sugimoto, Kodansha (Tokyo), 2004.
6 (*a*) M. R. Bryce, *Chem. Soc. Rev.*, 1991, **20**, 355; (*b*) T. Jørgensen, T. K. Hansen and J. Becher, *Chem. Soc. Rev.*, 1994, 41; (*c*) M. B. Nielsen, C. Lomholt and J. Becher, *Chem. Soc. Rev.*, 2000, **29**, 153; (*d*) J. L. Segura and N. Martín, *Angew. Chem., Int. Ed.*, 2001, **40**, 1372; (*e*) P. Frère and P. J. Skabara, *Chem. Soc. Rev.*, 2005, **34**, 69; (*f*) D. Canevet, M. Sallé, G. Zhang, D. Zhang and D. Zhu, *Chem. Commun.*, 2009, 2245.
7 T. Ishiguro, K. Yamaji and G. Saito, *Organic Superconductors*, 2nd edn, Springer, Berlin, 1998.
8 (*a*) X. Shao, Y. Nakano, H. Yamochi, A. D. Dubrovskiy, A. Otsuka, T. Murata, Y. Yoshida, G. Saito and S. Koshihara, *J. Mater. Chem.*, 2008, **18**, 2131; (*b*) X. Shao, Y. Nakano, M. Sakata, H. Yamochi, Y. Yoshida, M. Maesato, M. Uruichi, K. Yakushi, T. Murata, A. Otsuka, G. Saito, S. Koshihara and K. Tanaka, *Chem. Mater.*, 2008, **20**, 7551; (*c*) X. Shao, Y. Yoshida, Y. Nakano, H. Yamochi, M. Sakata, M. Maesato, A. Otsuka, G. Saito and S. Koshihara, *Chem. Mater.*, 2009, **21**, 1085.
9 (*a*) J. Sun, X. Lu, J. Shao, Z. Cui, Y. Shao, G. Jiang, W. Yu and X. Shao, *RSC Adv.*, 2013, **3**, 10193; (*b*) J. Sun, X. Lu, J. Shao, X. Li, S. Zhang, B. Wang, J. Zhao, Y. Shao, R. Fang, Z. Wang, W. Yu and X. Shao, *Chem.–Eur. J.*, 2013, **19**, 12517; (*c*) X. Lu, J. Sun, Y. Liu, J. Shao, L. Ma, S. Zhang, J. Zhao, Y. Shao, H.-L. Zhang, Z. Wang and X. Shao, *Chem.–Eur. J.*, 2014, **20**, 9650.
10 (*a*) J. Sun, X. Lu, M. Ishikawa, Y. Nakano, S. Zhang, J. Zhao, Y. Shao, Z. Wang, H. Yamochi and X. Shao, *J. Mater. Chem. C*, 2014, **2**, 8071; (*b*) X. Lu, J. Sun, S. Zhang, L. Ma, L. Liu, H. Qi, Y. Shao and X. Shao, *Beilstein J. Org. Chem.*, 2015, **11**, 1043.
11 S. Zhang, X. Lu, J. Sun, Y. Zhao and X. Shao, *CrystEngComm*, 2015, **17**, 4110.
12 L. Ma, J. Sun, X. Lu, S. Zhang, H. Qi, L. Liu, Y. Shao and X. Shao, *Beilstein J. Org. Chem.*, 2015, **11**, 850.
13 P. Guionneau, C. J. Kepert, G. Bravic, D. Chasseau, M. R. Truter, M. Kurmoo and P. Day, *Synth. Met.*, 1997, **86**, 1973.
14 L. Kloo, J. Rosdahl and P. H. Svensson, *Eur. J. Inorg. Chem.*, 2002, 1203.
15 S. Dolder, S.-X. Liu, E. Beurer, L. Ouahab and S. Decurtins, *Polyhedron*, 2006, **25**, 1514.
16 J. B. Torrance, J. E. Vazquez, J. J. Mayerle and V. Y. Lee, *Phys. Rev. Lett.*, 1981, **46**, 253.